

CHEMISTRY AND MINERALOGY OF THE MARGIN UNIT, JEZERO CRATER, MARS, OBSERVED BY M2020 / SUPERCAM. R.C. Wiens¹, E. Clavé², P. Beck³, C. Royer¹, C. Bedford¹, O. Beyssac⁴, C. Quantin⁵, T. Bosak⁶, A. Udry⁷, N. Mangold⁸, E. Dehouck⁷, S. Maurice⁹, A. Cousin⁹, O. Forni⁹, G. Caravaca⁹, A. Brown¹⁰, L. Mandon¹¹, J.R. Johnson¹², S.M. Clegg¹³, A.M. Ollila¹³, R.B. Anderson¹⁴, T.S.J. Gabriel¹⁴, P. Gasda¹³, J.I. Simon¹⁵, B. Horgan¹, F. Poulet¹⁶, C. Pilorget¹⁶, S. Connell¹, H. Manelski¹, S. Schröder², T. Fouchet¹⁷, J. Frydenvang¹⁸, O. Gasnault⁹, H. Kalucha¹¹, J. Lasue⁹, S. Le Mouelic⁸, G. Lopez Reyes¹⁹, J.M. Madariaga²⁰, G. Arana²⁰, J. Aramendia²⁰, I. Poblacion²⁰, J.-A. Manrique¹⁹, P. Pinet⁹, S.K. Sharma²¹, K. Stack²², K. Farley¹¹, and the SuperCam team ¹Purdue (rwiens@purdue.edu), ²DLR-OS, ³U. Grenoble, ⁴UPMC Paris, ⁵U. Lyon, ⁶MIT, ⁷UNLV, ⁸LPG Nantes, ⁹IRAP, ¹⁰Plancius Res., ¹¹Caltech, ¹²APL, ¹³LANL, ¹⁴USGS, ¹⁵JSC, ¹⁶IAS Orsay, ¹⁷LESIA, ¹⁸U. Copenhagen, ¹⁹U. Valladolid, ²⁰U. Basque Country, ²¹U. Hawaii, ²²JPL

Introduction: The *Margin Unit* of Jezero crater, Mars, was identified from orbit as one of the most carbonate-rich regions of the planet [e.g., 1,2]. Its presence, along with the adjacent fluvial delta [e.g., 3] made Jezero crater the most compelling landing site for the Mars 2020 mission [4]. Investigation of Jezero's Margin-Unit carbonates provides a unique opportunity to address the formation of carbonates in sedimentary deposits, possibly under a CO₂-rich martian atmosphere. Here we report on chemistry and mineralogy of 55 targets observed by the multi-technique SuperCam instrument during Perseverance's crater-margin campaign.

Traverse: Fig. 1 shows the location of the Margin Unit relative to the western delta to the east and the crater rim. Topographically, the unit is generally higher than the delta, and the main channel of Nereitva Vallis bisects it. The Margin Unit thus pre-dates at least the upper part of the delta. Perseverance has been exploring the Margin Unit since Sol 910 (11-Sep-23). After exploring and collecting a sample [5] at Hans Amundsen (HA) Memorial Workspace (named for a team member who passed away in 2023), the rover drove up a delta lobe and re-entered the unit on Sol 927 to investigate Turquoise Bay (TB), a region where the orbital carbonate signal is especially strong [2]. After collecting a sample [5], Perseverance crossed the lobe and re-entered the unit to explore a region called Gnaraloo Bay (GB). We report here on the region west of the lobe (white box in Fig. 1), dominated by the HA workspace and the TB region.

Carbonate Observation Methods: Mineral interpretations from infrared (45 targets) and Raman (6) spectra, and elemental compositions from LIBS (42 targets) were obtained by SuperCam. The primary carbonate detection in SuperCam's IR range (1.3-2.6 μ m) is based on simultaneous observation of 2.3 and 2.5 μ m absorptions. However, the 2.3 μ m absorption by itself may indicate other Fe/Mg-phylllosilicates. Modeling of the IR spectra indicates that SuperCam's detection limit for Mg-Fe carbonates can vary significantly depending on the constituents of the mineral mixtures and grain sizes. Raman spectra were

taken in abrasion patches in HA and TB as well as on natural surfaces. Raman observations of natural surfaces tend to have much weaker signals, likely due to surface roughness and significant UV [6,7] and other radiation exposure. LIBS has relatively high (> 10 wt%) detection limits of carbonate due to signal from CO₂ in the martian atmosphere. A secondary indicator of carbonates with LIBS in the absence of sulfates or phosphates is low abundances of SiO₂, e.g., < 35 wt%.

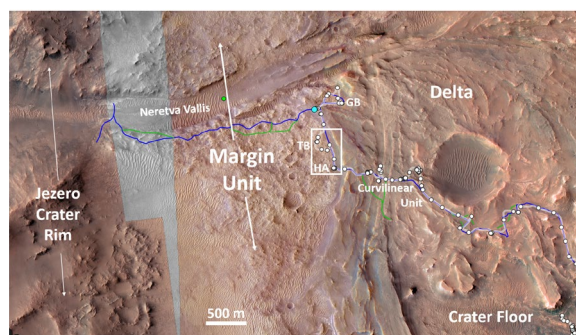


Fig. 1. Location of the Margin Unit between Jezero's crater rim and delta. Gray trace indicates rover path with stops (white dots); blue is anticipated path. White rectangle indicates area described in this study.

Results—Elemental Compositions: SiO₂ abundances in the Margin Unit (shown with C detections in Fig. 2) are bimodal, with peaks below 20 wt % and in the 40-50 wt % range. There is also a significant tail toward high (> 65 wt %) SiO₂. One float rock, AEGIS 910, appears to be nearly pure hydrated silica [8]. High-silica observations in bedrock are frequent, although never uniformly high over even several millimeters. FeO_{tot} and MgO mean abundances are 25.8 and 21.9 wt %, resp., indicating strong mafic contributions. These elements are generally anticorrelated with SiO₂, suggesting Fe/Mg carbonates. Al₂O₃, CaO, and Na₂O are relatively low, although a slight correlation among these elements suggests a contribution from plagioclase in the local rocks. Relative to previous portions of the traverse, somewhat more carbonates and high-silica points are inferred in the Margin Unit, although the curvilinear portion of the delta just to the east (Fig. 1)

showed nearly as many [9]. Within the Margin Unit, HA and TB have similar mean compositions. SiO₂ abundances vs. depth are steady in C-rich targets, indicating that the carbonates are not merely weathering coatings.

Results—IR Spectra, Raman, & Inferred Mineralogy: Raman spectra provide unequivocal confirmation of carbonates in the two abrasion patches in the Margin Unit, in agreement with other instruments [5,10,11]. Mg #s (~30-55) are toward the lower end of the range observed in other portions of the traverse. Infrared spectra likewise indicate relatively abundant carbonates, but not more so than the Curvilinear Unit explored just prior to the Margin Unit. The presence of other clay minerals is apparent from 1.9 and 2.4 μ m bands present in most spectra, even though carbonate absorptions can mask the phyllosilicate contributions to the 2.3 μ m band. Overall, the phyllosilicate abundances seem slightly more muted in the Margin Unit. The carbonates are almost always associated with a hydrated silica spectral signature (e.g., 2.2 μ m band).

Texture & Morphology; Soils: Ridges and sulfate- and CaF₂-rich veins were observed in the TB area [12, 13]. Patterns with concentric circles at the meter scale were seen at HA (Fig. 3a). Targets at 3 radial distances hinted at decreases in major-element abundances with radius, but differences were not significant.

Bedrock textures in the Margin Unit display increased roughness, especially at TB (Fig. 3c). Coarse-grain soils in the area have strong IR carbonate signatures. Grain sizes average ~2 mm (Fig. 3b). Close inspection of the roughest bedrock targets suggests that ~2 mm gray grains, potentially corresponding to the soil carbonate grains, appear to be weathering out of a lighter matrix in the bedrock (Fig. 3c inset).

Discussion: The appearance of mm-size carbonate grains apparently weathering out of the bedrock suggests a distinctly different (detrital) origin than carbonates in Seitah, which has thin carbonate rinds at grain boundaries and interstitially, indicative of authigenic weathering [14]. Olivine sands are known to occur in the Nili Fossae region [15] and could have resulted from pyroclastic deposition [16] and subsequent weathering. Interaction of millimeter-size olivine grains with water at a moderate pH and saturated with CO₂ could result in replacement of these grains

with Mg-Fe carbonates and other phases. This could have occurred during the highest stands of Jezero lake, prior to excavation of the outflow channel, as beach deposits [17]. Another potential hydration source is groundwater. Olivine sand may have been emplaced via a mass wasting event, or it could have collected as dunes during a dry period, or on an ice-covered region that subsequently melted. Return of samples collected in the Margin Unit as well as continued exploration with Perseverance will provide further insight into this more ancient Jezero crater unit.

Acknowledgement: We thank NASA, CNES, and other funding agencies for their critical support.

References: [1] Ehlmann B.L. et al. (2008) *Science* 322, 1828. [2] Horgan B.H.N. et al. (2020) *Icarus* <https://doi.org/10.1016/j.icarus.2019.113526>. [3] Fassett C.I. and Head J.W. III (2005) *GRL* doi:10.1029/2005GL023456. [4] Grant J.A. et al. (2018) *PSS* 10.1016/j.pss.2018.07.001. [5] Siljestrom S. et al., this meeting. [6] Royer C. et al. (2024) <https://doi.org/10.1016/j.icarus.2023.115894>. [7] Clavé E. et al. (2024) subm. [8] Beck P. et al., this meeting. [9] Clavé E. et al., this meeting. [10] Horgan B. et al., this meeting. [11] Hurowitz J. et al., this meeting. [12] Poblacion I. et al., this meeting. [13] Wolf Z.U. et al., this meeting. [14] Farley K.A. et al. (2022) *Science*, 10.1126/science.abo2196. [15] Mandon et al (2020) <https://doi.org/10.1016/j.icarus.2019.113436>. [16] Ruff S. (2022) <https://doi.org/10.1016/j.icarus.2022.114974>. [17] Jones A.J. et al., this meeting.

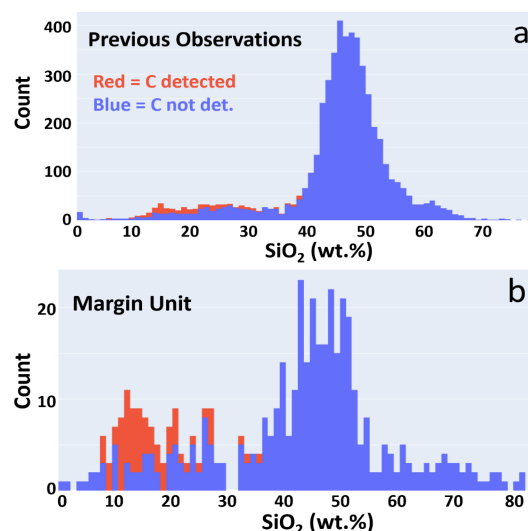


Fig. 2. Histogram of SiO₂ abundances, with and without C detections, in the previous portion of the mission (a) and in the Margin Unit (b).



Fig. 3. a) Concentric feature at Amundsen (Mastcam-Z). b) Carbonate-rich coarse-grain soil target Toothawara (RMI). c) Rough texture of Baresand Point target at Turquoise Bay (RMI). Inset shows darker grains similar in size to the soil grains, apparently weathering out of bedrock.